Understanding and Quantifying the Role of Polyethylene Photodegradation in Altering Protein Adsorption.

A Thesis

SUBMITTED TO THE FACULTY OF THE

UNIVERSITY OF MINNESOTA DULUTH

BY

Liam Paul Fawcett

IN PARTIAL FULFILMENT OF THE REQUIREMENTS

FOR THE DEGREE OF

MASTER OF SCIENCE

Melissa Maurer-Jones, Adviser

August 2021

Acknowledgements

I would like to acknowledge the University of Minnesota Duluth's Department of Chemistry and Biochemistry for funding this project.

Special thank you to Dr. Melissa Maurer-Jones and Dr. Margaret Elmer-Dixon for all of their assistance with analysis and ideas for data collection. As well as helping to prepare me as much as possible for the next steps in my professional development.

To my group members, especially Thea, Jonathan and Emma for their help with data collection and pushing me to the finish line.

Finally, to my family for their love and support during my time working to achieve my goal.

Abstract:

Due to its desirable physical and chemical characteristics and low production costs, plastics have become an extremely desirable product for both industrial and consumer purposes. However, due to these same desirable characteristics and improper disposal avenues, plastics have become an environmental concern, particularly their impact on ecosystems. Once plastics enter the environment, there are synergistic driving forces that cause weathering. While many of the degradation pathways of polymers in the environment are well documented the interplay between abiotic and biotic degradation are not well understood. In this work, the role of polyethylene's photodegradation on protein adsorption are investigated. Protein adsorption is a key step in biofilm formation and biotic degradation of polymers. This work specifically focuses on the model protein BSA and its adsorption to PE. Through investigative spectroscopic techniques (i.e., fluorescence and circular dichroism), it was shown that an increase in hydrophilicity caused by photodegradation of the polymers' surface, caused less perturbation of the local environment of the tryptophan residues. It was also observed that there was larger structural frustration and rearrangement of the protein upon binding to PE at points during photodegradation, where there were significant changes in the chemical and physical properties. Depending on the inherent protein stability, larger structural changes upon surface binding indicate an increase in adsorption strength. Environmentally, this

signifies an increase in biofilm strength at the transition points in polymer photodegradation leading to a potential increase in the rate of biodegradation.

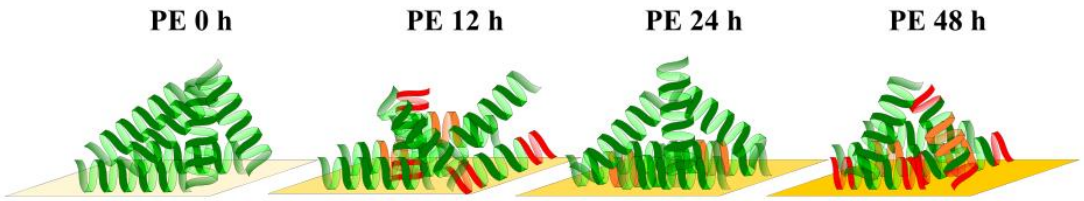

Contents

List of Tables

List of Figures

Chapter 1 : Photodegradation of plastics and its role in changing protein adsorption

1.1 Introduction

After the introduction of the first synthetic plastic, there has been a massive demand to increase their production for both industrial and commercial purposes due to their low cost and desirable properties. As the demand and use of plastics change, a significant amount of newly synthesized plastics have been developed and placed into production. The trend of industry switching from more expensive materials to the cheaper lightweight plastics is demonstrated by the sheer mass production of polymers. In 2019 alone, there was 368 million metric tons of plastic produced and the trends indicate that yearly production will only increase (Geyer et al., 2017).

While there are many industrial uses for plastics, the majority of production is for commercial purposes, mainly for single use plastics such as bags or straws. Of the produced plastic, only 8% is recycled because of various factors (EPA, 2021). This means that 92% of the plastics produced are managed within the waste stream (i.e., are incinerated or landfilled). Unfortunately, there can be mismanagement of waste, that ultimately leads to the dispersion of plastics through the environment. Although plastics are desirable due to their physical and chemical properties, those same properties cause plastics in the environment to pose various risks, which has become a main focus of environmental research since it was brought to attention in the mid 1960's (Thompson et al., 2009).

1.2 Plastics in the Environment

After entering the environment, the plastics can be transported by the wind and water to larger aggregation points called sinks. These sinks span across various

ecosystems; however, the impact on their surroundings is incredibly evident. One of the most apparent impacts of the plastics that have entered the environment is the formation of a "plastisphere" or an ecosystem that has evolved to survive on and around human-made plastics (Amaral-Zettler et al., 2020). Although biotic degradation of the polymers can occur, it does not occur fast enough to sustain life. Due to the longevity of the polymers surface, it can collect and transport enough nutrients that would otherwise be limiting in the ocean to sustain life in this ecosystem (Roman et al., 2020). This has led to large self-sustaining ecosystems at the accumulation centers (Lebreton et al., 2018).

While the plastics can act as vectors for nutrient that are necessary for survival, the plastics also have some severely detrimental effects on the survival of many organisms. For instance, many charismatic macrofauna (i.e., birds and fish) can often mis-identify the colorful plastics as food and ingest them. This leads to a feeling of satiation without obtaining any nutrients eventually leading to starvation. Plastics have also been found in other organisms such as filter feeders leading to effects such as changes in reproductive activity and lessened O_2 consumption (Hermabessiere et al., 2017). The plastics also can act as a vector and site for accumulation of toxic pollutant molecules that would otherwise be at less harmful concentrations due to their dilution (Amelia et al., 2021). For example, Velzeboer et. al. have shown that hazardous organic compounds such as polychlorinated biphenyl's and polycyclic aromatic hydrocarbons can sorb to the surface of microplastics and eventually transfer to organisms (Velzeboer et al., 2014). Beyond chemical toxicants, studies have even shown that the plastics can transport harmful algae or other species that would otherwise not survive as their natural substrate, kelp or other plant life, would eventually disintegrate (Masó et al., 2003).

The degree to which plastics act as a substrate for chemical and biochemical attachment can be related to their weathering (Kedzierski et al., 2018; Liu et al., 2020; Sun et al., 2020). Weathering means that as plastics are transported through the environment, they are exposed to numerous environmental factors that can begin to alter their physical and chemical characteristics eventually leading to their degradation. These factors are grouped into two categories, abiotic degradation pathways or biotic pathways, and are explored in more depth below.

1.3 Degradation of plastics

Largely due to their robust backbone structures, traditionally-designed plastics (e.g., polyethylene and polypropylene) remain in the environment for extended periods of time. Even in industrial settings, plastics are most often incinerated because there are no methods currently developed to efficiently break them down into their monomers (Verma et al., 2016). While in the environment and over time, plastics are exposed to the various stressors that cause chemical and physical transformations. It must be noted that although these pathways are discussed below as separate categories, these are a synergistic processes that influence each other to further the degradation of the polymer in the environment.

1.3.1 Abiotic degradation pathways

Abiotic degradation refers to pathways that rely on non-biological changes to the polymer backbone rather than biologically induced changes to the backbone structure. The primary pathways of abiotic degradation are generally classified as either thermal, mechanical, or photochemical. Although, mechanical and photochemical degradation pathways are typically the most environmentally relevant, particularly in aqueous environments (Gewert et al., 2015). The primary focus for this work will be investigating

the photodegradation pathways roles in influencing biotic degradation to occur and will therefore be discussed in greater detail below.

Photodegradation: Pathways and Products

While the specific mechanisms depend on the polymer, photodegradation generally follows three major pathways demonstrated in Figure 1.1: crosslinking, oxidation, and scission (Maurer-Jones & Monzo, 2021; Shyichuk & White, 2000).

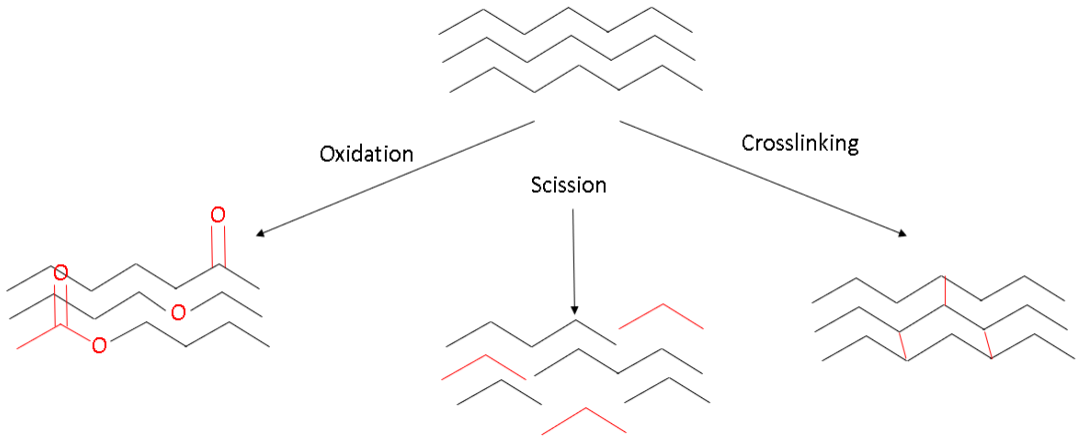

Figure 1.1: Proposed polyethylene photodegradation pathways. Black lines represent polymer backbone and red lines represent photoinduced chemical transitions to the polymer.

Oxidation

This diffusion-controlled process occurs in the presence of oxygen and light leading to the formation of oxygen moieties on the surface of the polymer. Typically, the initiation of these reactions rely on impurities imbedded within the backbone of the polymer generated during the manufacturing process(Allen & McKellar, 1975). The formation of the oxygen groups on polymer surfaces is proposed to proceed through a

series of radical reactions eventually leading to the formation of ketones or aldehydes depending on their location (Gardette et al., 2013).

Tracing of the formation of these functional groups is typically done through the usage of attenuated total reflectance Fourier transform infrared spectroscopy (ATR-FTIR). Unlike classical FTIR, this technique only monitors the surface of the plastic. One common method for quantifying the degree of oxidation is to monitor the changes in area to the carbonyl band (1660-1760 cm^{-1}) that are normalized to a non-changing polymer backbone band (1395 cm^{-1}). This value is often used within the materials science community and is known as the carbonyl index (ASTM F2102-17).

Crosslinking

The formation of radicals along the polymer backbone through light induced reactions can also cause branching across adjacent macromolecules. While the predominant degradation pathway under oxic conditions is oxidation, the crosslinking pathway is the primary pathway for photodegradation under anoxic conditions (A. Singh, 1999). Crosslinking of the polymers backbone induces changes to the mechanical properties of the polymer which overall increases brittleness and changes the melting point (Gao et al., 2002). A common method to assess crosslinking is quantifying the insoluble fraction of the polymer in organic solvent, where insolubility increases with crosslinking. However, this becomes a difficult measurement on polymers that have high insolubilities to begin with (e.g., polyethylene) (Kujirai et al., 1968).

Scission

Scission reactions cause cleavage of the polymer backbone into fragments of lower molecular weights. The most predominant scission reaction pathways are the Norrish type I and II reactions, where radicals are formed by either hydrogen abstraction (Type II) or α-cleavage (Type I) around ketones formed through oxidation (Ansyln & Dougherty, 2006). These cleavage reactions cause increases in the crystallinity of the polymer, overall decreasing the likelihood of biotic degradation to occur (Chamas et al., 2020).

The main methods for tracking scission is looking at the molecular weight of solubilized polymers with gel permeation chromatography (Tomer et al., 2012). Additionally, scission, and crosslinking to a lesser extent, can be monitored indirectly. Differential scanning calorimetry (DSC) is a method that monitors the changes of crystallinity, which is expected to change as the result of these reactions, through the changes in heat required to raise the temperature of the sample. ATR-FTIR can again be utilized for characterization of these reactions by monitoring a polymer specific peak related to the crystalline phase transition (Lanyi et al., 2018). This however has its own challenges when sampling polymers independent of lab induced natural environments as irreversibly adsorbed particles on the surface can interfere with the signal.

Overall, the primary products of these pathways result in increased oxidation of the surface, changes to the crystalline structure of the polymer, and fragmentation into chains of smaller molecular weight (Rabek, 1995). These changes to the polymers backbone structure ultimately influence the availability and progression of biotic degradation pathways.

1.3.2 Biotic Degradation

As stated above, plastics found in natural systems have booming populations of microbial communities formed on their surfaces, commonly referred to as the plastisphere (Amaral-Zettler et al., 2020). These plastics act as vectors for what would otherwise be limiting nutrients in the ocean (e.g nitrogen, phosphorus and iron), making it desirable for the microbial species to interact with the polymers eventually leading to their biotic degradation (Roman et al., 2020). While not required, many times the initial phases of biotic degradation begin with the formation of a biofilm on the polymers surface (Lobelle & Cunliffe, 2011). Biofilms form as a mechanism for the microbes to protect themselves against xenobiotics, but also enables microbial species to participate in a group metabolism. This allows for the breakdown of materials that would otherwise be difficult to mineralize. (Donlan & Costerton, 2002; S. Singh et al., 2017).

1.4 Biofilm Formation

Formation of biofilms on the surfaces directly impacts the fate of the polymers through a process called biofouling, in which the extracellular polymeric substances generated from the microbial species present cause an increase in density making the polymer sink (Kaiser et al., 2017). Biofilm formation can be further broken down into four distinct stages: adsorption, grown, production of extracellular polymeric substances (EPS) and finally motility.

1.4.1 Adsorption

The initial step of biofilm formation is the adsorption onto the surface. This is a highly complex process that requires both bio-specific/selective and non-specific (hydrophobic or electrostatic) processes (Rabe et al., 2011). Typically, the non-specific repulsion forces must first be overcome. When forming biofilm layers on hydrophilic

surfaces, the bacteria will use specific intermembrane amphipathic anchor proteins called adhesins (Berne et al., 2015). These interacting and adhering proteins form a macromolecular biomolecule layer on the surface that helps to establish a connection between the cell and the polymer and overcome any superficial hydrophobic repulsive forces (Donlan, 2002). Once the repulsive forces of the surface have been overcome, electrostatic interactions are established reinforcing the binding between the polymer surface and the cell. While biofilm formation can be initiated on both hydrophobic and hydrophilic surfaces, a study by Katsikogianni et al. validated a thermodynamic model that demonstrated that the surface characteristics of both the substrate and bacteria are contributing factors to adhesion (Katsikogianni et al., 2004). These findings suggest that as the surface changes due to photodegradation may attenuate the extent and strength of polymer-cellular interactions. Although biofilms may form on most surfaces, studies have shown that the formation of a protein layer on the interaction surface is generally a prerequisite to the adherence of cells at that site (Kalasin & Santore, 2009). This formation of a protein layer is an extremely complex process and understanding how the proteins interact with the surface relies on a multitude of factors that will be explored in greater detail below.

1.5 Proteins and their structures

Proteins are unique biopolymers composed of varying amounts of the 20 standard amino acids. These amino acids are organic molecules containing an amino group, a carboxylic acid, and differentiating R-groups attached to a chiral carbon. When building a protein, these amino acids are linked together through a hydrolysis reaction. As the protein folds, the R-groups protruding off the amino acids are oriented to protrude outwards helping to derive the proteins structure and function. In living cells, these

proteins each have individual functions that when grouped together will provide the organism with the necessary nutrients/molecules needed for survival (O'Connor & Adams, 2010). Proteins structures are unique to their function but can be broken down into four categories: primary, secondary, tertiary, and quaternary structures. The primary structure is the sequence of amino acids that comprises the protein itself, this unique pattern will, when folded correctly, lead to an active protein that can perform its specific task within the cell. The secondary structure is how the primary sequence of amino acids fold together to form structural characteristics. The most commonly observed of these structural characteristics is the alpha-helix and β-sheet. As the structures begin interacting, they start to form motifs such as two β-sheets being linked together by an alpha-helical structure. As more and more of these motifs are formed, the protein begins to form its tertiary structure. This structure is how these motifs interact to form the 3-dimensional structure in space. This structural formation is pertinent to how the protein functions, where incorrect folding of the tertiary structure (or loss of tertiary structure) can be detrimental to the protein's purpose such as loss of enzymatic function or initiation of disease through plaque (Moreno-Gonzalez & Soto, 2012). The quaternary structure relates to how smaller protein subunits come together to form a functional macromolecule (O'Connor & Adams, 2010).

Protein folding is driven by a series forces that cause the amino acid to orient in a specific directions. Two of the major driving forces behind protein folding are the hydrophobic interactions and hydration of the surface (Pace et al., 2015). While these two forces are dominant, there are other molecular driving forces that influence protein folding. Within the cell, there are various levels of salinity that drives the amino acids

charges to be changed dependent on how folding proceeds. These interactions have to do with electrostatic forces and drive the overall proteins charge (Martins de Oliveira et al., 2018). In an example of electrostatic forces driving structure, extending the pH too far pas a proteins isoelectric point (i.e., the pH where the overall charge of the protein is neutral) in either direction can lead to loss of protein structure (Schuurmans Stekhoven et al., 2008). These driving forces lead to the secondary and/or tertiary structural characteristics to be formed which are necessary for both the function and location of the protein (Deller et al., 2016).

Alpha-Helix and its structure

The alpha-helix is a common secondary structure comprised of amino acids that are connected by hydrogen bonds. These hydrogen bonds are formed from the carbonyl oxygen group (*i*) of the backbone amino acid accepting a hydrogen from the amide (*i+4*) (Eisenberg, 2003). Due to the stereochemistry of the amino acids, these structures form righthanded spirals with approximately 3.6 amino acids per turn giving them their common name 3.6-helicies (alpha-helix seen represented in Figure 1.2). The R groups protruding off of the amino acid backbones face outwards as to not interfere with the spiral formation (Lodish et al., 2000). Depending on their final destination within the cell, the helices are polar, non-polar or amphipathic. For example, a helix which is embedded

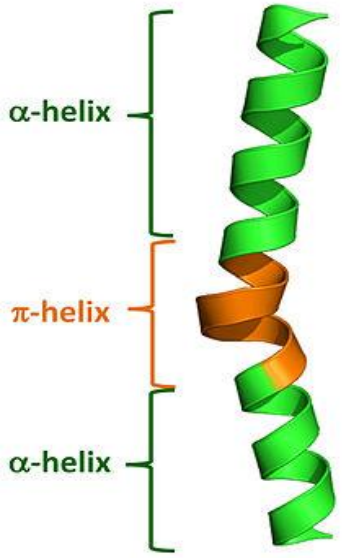

Figure 1.2: Representative image of difference between 3.6 and Π helical structures (Cooley et al., 2010).

in a membrane will most likely be non-polar in nature to ensure that it remain embedded, where-as a helix on the exterior of a free-floating protein will be amphipathic.

Outside of the normal 3.6-helicies, there are also two additional conformers that can form. The first, known as the 3.10-helix, is a more tightly wound structure typically seen at either end of the helical structure and not stable on its own. This structure has hydrogen bonds at *i* and *i+3* getting its name from having 10 atoms separating each donor acceptor pair rather than the normal 13. The second is the Π-helix (Figure 1.2 orange), where hydrogen bonds are separated by *i* and *i+5*.It is not normally observed due to the spacing down the interior of the (Cooley et al., 2010; Creighton, 2010). Figure 1.2 shows a Π-helix with no appreciable length demonstrating that the backbone orientation of the amino acids dictates its secondary structure, not the outward appearance of the amino acids.

Beta-Sheet and its structure

Another common secondary structure is the beta-sheet, which is composed of a series of beta-strands linked together by hydrogen bonds. beta-strands are not stable as a standalone unit, and therefore are only stabilized when in a sheet formation. The R groups protruding off of the amino acids in a beta sheet alternate between facing upwards and downwards. Depending on the layout of the strands within the sheet, there are two commonly seen structures that are

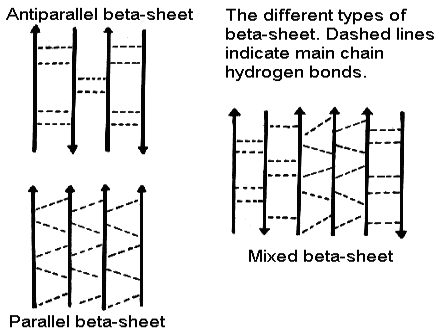

Figure 1.3: Depictions of Beta-sheet structures that can occur. (Krejchi et al., 1997)

formed: parallel sheet, and antiparallel sheet. In the parallel sheet, the strands run parallel to each other, and hydrogen bonding occurs at angles to the adjacent strand. In the antiparallel sheet, the strands run opposite of each other, and hydrogen bonding occurs perpendicular to the adjacent strands shown in Figure 1.3 (Berova et al., 2012; Krejchi et al., 1997).

1.5.1 Monitoring Protein Secondary Structure

Through advances in technology, the ability to monitor proteins secondary and tertiary structure has become more and more precise. Quantifying and identifying how proteins fold is incredibly important in understanding their enzymatic function, role in disease state, and even how they interact with each other in the cell (Sneha & Priya Doss, 2016). Currently, there are many techniques that can be utilized to identify the secondary structures of a protein in both free solution as well as its crystalline form.

Solid State Techniques

Solid state techniques, used to determine secondary structural characteristics of proteins and their complexes, rely on fixation of the protein into a crystalline form. That means the predicted structures might not be enzymatically relevant. Generally, these techniques are used to identify larger macromolecular complexes ,such as amyloid plaque formation or keratin fibrils. However, some techniques can be used to determine structural characteristics of individual proteins clustered together.

Transmission electron microscopy (TEM) uses a beam of electrons to identify structural characteristics of protein sample (Spillers et al., 2017). By detecting the transmitted electrons, the secondary structures can be elucidated, although at relatively

low resolution. X-ray diffraction (XRD) utilizes X-ray incident beams diffraction patterns through a crystalline structure to accurately determine structural characteristics of a protein packed crystal (Parker, 2003). Attenuated total reflection Fourier transformed infrared spectroscopy (ATR-FTIR) utilizes adsorption of infrared light to elucidate the secondary structure of a protein. As proteins are typically in hydrated environments, which adsorb strongly in this region, the protein must be locked in a crystalline structure that again does not necessarily represent the most enzymatically active structure. However, using the bands associated with the secondary structures, predictions can be made to accurately describe the structure in its crystalline form (Sukumaran, 2018).

Solution Techniques

Unlike solid state techniques, solution techniques provide enzymatically relevant structural characteristics of a protein. While these techniques can be limited by the size of the protein, the structural relevance of the findings can reveal insights into how the proteins interact within their native conditions.

Nuclear magnetic resonance (NMR) is a currently rising powerful technique that can be used to identify secondary structures of proteins in solution (Cavalli et al., 2007). Although relatively new, this technique allows for identification of the secondary structure of a protein in its native state, in solution, rather than an entropically idealized state that may not be enzymatically relevant. This technique is limited, however, to quantifying smaller proteins or isolated subunits, with current size limitations of 39 kDa or smaller for accurate results (Gauto et al., 2019). As the secondary structures of proteins are chiral in nature, circular dichroism (CD) can be used to accurately determine

structural characteristics of proteins. CD uses circularly polarized light to identify the structural characteristics of the protein (Berova et al., 2012). Atomic force microscopy (AFM) monitors changes to surface topology through the usage of a spring-like cantilever. (Pleshakova et al., 2018). Whited & Park used this method to determine high-resolution structural characteristics of single protein molecules in lipid bilayer locked proteins (Whited & Park, 2014).

Although these are just a few of the methods used to determine secondary structures, they can provide an accurate representations of the secondary structure while also enabling predictions of the protein's tertiary structure. However, upon adsorption to a given surface, these structures will begin to shift, and depending on the surface to which the protein is binding, many of these methods will no longer be applicable for determination of protein's secondary structures.

1.6 Protein Adsorption to Solid Surfaces

Understanding how proteins interact with the solid surfaces is incredibly important for a multitude of different fields. For example, investigating deterrence of protein adsorption in prosthetics can lead to decrease of infection rates, or understanding and directing the orientation of proteins on a membranes utilized for immuno-assays is necessary for their functionality (Lebaron & Athanasiou, 2000; W. Zhang et al., 2011). However, not much is understood regarding the adsorption of proteins onto plastics in the environment; specifically, not much is understood about how protein adsorption changes as the polymers in the environment undergo degradation and how this may influence further degradation of the polymers.

Protein adsorption is influenced by a multitude of factors at both the local and bulk environment. Local environmental factors that influence the ability for a protein to bind onto a given surface include but are not limited to electrostatic attraction, Vander Waals forces, and hydrophobic interactions in both the protein as well as the surface to which it is binding (Rabe et al., 2011). Within the bulk environment, there is competitive binding between proteins in solution where binding of certain proteins can deter binding of other proteins. Protein concentration in solution can also influence protein adsorption and orientation upon adsorption (Thyparambil et al., 2015). However, it is generally accepted that the driving force behind the adsorption of proteins is related to an increase in the entropy from the release of water and salts adsorbed on the surface as well as conformational rearrangement of the protein upon adsorption (Ratner et al., 2012).

As proteins adsorb onto a surface, they can undergo conformational changes that can both effect their structure and potentially influence their function. Generally, proteins can be categorized as either “hard” or “soft” proteins. This classification relates to the overall structural changes that the proteins will undergo while adhering to any given surface. “Softer” proteins, such as bovine serum albumin (BSA), will undergo extensive conformation changes upon adhering to the surface (Felgueiras et al., 2018). This can include partial unfolding of the protein, potentially to the extent that it loses is enzymatic capabilities (Hlady & Buijs, 1996). Harder proteins on the other hand generally do not undergo conformational changes when binding to any given surface and usually rely on electrostatic attractive forces to induce adsorption onto the surface.

1.6.1 Thermodynamics of protein adsorption onto solid surfaces

Conformational changes of the proteins as they adsorb onto the surface are generally related to the overall internal stability of the protein. This can be related back to the thermodynamics of the system. For a conformational shift to occur there must be some sort of gain in conformational entropy (Ratner et al., 2012). For softer proteins, this change in conformational entropy usually is indicative of irreversibility of binding; however, proteins that can bind reversibly that undergo the large conformational shifts usually will not return to their natural conformation upon unbinding. The harder proteins, due to their rigidity, usually need electrostatic attractive forces to induce binding onto the surface (Felgueiras et al., 2018). This indicates that if there are changes to the charge of the surface towards that of opposite of the protein, there will be more protein that binds.

1.6.2 Monitoring Changes to Protein Structure Upon Surface Binding

Once the proteins interact with the surfaces many of the techniques that could be used to describe their secondary structures are unable to capture relevant structural information due to interference from the surface they are adsorbed to. However, as the proteins adsorb onto the surface, other techniques can be utilized to gain an understanding as to the changes in structural characteristics of the proteins.

Fluorescence characterization

Within the proteins, there are a few amino acids that fluoresce when excited by certain wavelengths of light. These are the aromatic amino acids including tryptophan (W), tyrosine (Y) , and phenylalanine (F). Both tyrosine and phenylalanine have extremely weak fluorescent signals that are heavily influenced/quenched by their local environment. Tryptophan, on the other hand, has a strong fluorescent signal and while it

is influenced by its local environment, the signal can always be observed outside of the presence of a quencher (Hsieh et al., 2016).

Using fluorescence to monitor changes to structure upon binding to a surface does not directly lead to understanding changes to the secondary structures, but rather yields information regarding the environment of the tryptophan residues within the protein (Royer, 1995). The exact ways this can be monitored will be explored in more detail in chapter three of this work.

Circular Dichroism Characterization

Alternative techniques

Many of the techniques described above can provide useful information regarding the secondary structures of adsorbed proteins. ATR-FTIR, for example, may provide critical information regarding the changes to the secondary structures. Yet, if there are interfering signals due to the background surface, parsing out the small changes to the structures becomes extremely difficult if not impossible. If the surface to which the proteins are adsorbing are transparent to circularly polarized light, CD offers extremely detailed information regarding changes to the secondary structure upon adsorption. Unfortunately, techniques such as AFM and XDR no longer provide more useful information when characterizing proteins adsorbed to surfaces as the surface interferes with the signals too much and characterizing the small changes will become impossible. For this reason, this work will focus on utilizing CD and fluorescence spectroscopies.

1.7 Summary and Objectives

As the plastics that have entered the environment begin their degradation processes, understanding how the abiotic degradation pathways influence how microorganisms interact with the polymers surface is important in determining the overall fate of the polymers. Specifically, understanding the role that changes to surface level chemistry has on the binding and overall structural deformation of proteins can begin to elucidate the biofilm's binding strength and the potential for biodegradability of the plastics. This work will focus on the role in which photodegradation plays on the adsorption of a model protein bovine serum albumin (BSA) in to polyethylene (PE), one of the most prevalent polymers in aquatic plastic debris (Issac & Kandasubramanian, 2021). The changes to the structural characteristics of the protein will be monitored using CD and fluorescence spectroscopies. We hypothesize that the hydrophobicity of the polymers, which decreases with irradiation time, will drive changes in the protein structure because it is known that hydrophobicity and hydration are key factors in protein folding and structure (Hebner & Maurer-Jones, 2020; Maurer-Jones & Monzo, 2021). For these reasons, we hypothesize:

1. Photochemical degradation increases hydrophilicity of the polymer leading to less structural deformation upon binding for adsorbing 'soft' proteins such BSA, as observed by a smaller shift in the lambda max of the fluorescence with increasing irradiation time, because the local environment of the tryptophans when adsorbed to the polymer will more closely resemble the local environment when in free solution.
2. Less photochemically degraded polyethylene (i.e., more hydrophobic) will cause large changes to the secondary structures of adsorbing 'soft' proteins as

hydrophobic surfaces will cause dehydration of the proteins surface, which will lead to reorientation of the protein structures as demonstrated by shifts in the CD signals for alpha helical structures.

Chapter 2 : Materials and Methods

2.1 Polymer Photodegradation

Low density polyethylene (LDPE) 30 μm films were purchased from Goodfellow Cambridge Limited (Huntingdon, UK) (see Table 2.1 for summarized polymer film properties)

Table 2.1. Polymer film properties (Goodfellow, 2021)

Polyethylene	
Density (g/cm^3)	0.92
Refractive Index	1.51
Specific Heat (J/K kg)	1900-20300
Thickness (mm)	0.03

Films were mounted on cardstock and irradiated in a Rayonet merry-go-round photoreactor (Southern New England Ultraviolet Corp, Bamford, CT) using 16 Hg vapor lamps for exposure with 254 nm light. Polymer films were irradiated for either 12, 24 and 48 h on both sides to ensure uniform degradation.

2.2 Polymer Characterization

2.2.1 ATR-FTIR

Irradiated films were scanned and analyzed using a Nicolet iS510 FTIR spectrometer (Thermo Scientific, Waltham, MA) with a diamond crystal ATR scanning 600-4000 cm^{-1} with a resolution of 4 cm^{-1} and scan averaging of 64 scans per spectra. Backgrounds were taken prior to each new scan and the film was sampled in at least 3 different locations to ensure uniformity of the photochemical transformation over the

film's surface area. All spectra were acquired using OMNIC software in triplicate (Thermo Scientific, Waltham, MA) .

2.2.2 Differential Scanning Calorimetry (DSC)

Thermograms of irradiated polymers were collected on a Discovery 250+ DSC (TA Instruments, New Castle, DE). PE samples were cycled from 10 ^{o}C to 180 ^{o}C at 10^{o}C/min in a heat, cool, heat cycle. The two separate heating cycles were used to minimize error that might be caused by the loading of the thin films.

The melting peak was integrated within the Trios software (TA Instruments, New Castle, DE), and the peak temperature and enthalpy values were recorded. Enthalpies were converted to a percent crystallinity using the value of 293 J/g, a value reported in the literature for 100% crystalline sample (Blaine). Triplicate samples were analyzed, and the crystallinity values reported as averages ± standard deviation.

2.3 Protein Adsorption Characterization

2.3.1 Bovine Serum Albumin Standard

Lyophilized BSA (98%) was purchased from Sigma Aldrich (CAS:9048-46-8, St. Louis, MO). Solutions were prepared in a 0.01 M sodium phosphate buffer at pH 7 using 8 g NaCl (Fischer Chemical, Waltham,MA), 200 mg KCl (Fischer Chemical, Waltham, MA), 1.44g Na_2HPO_4 (Acros Organics, Fair Lawn, NJ), 240 mg NaH_2PO_4 (Fischer Chemical, Waltham,MA) per liter of double distilled water. BSA solutions were 0.048 mg/ml for fluorescence experiments and 0.5 mg/ml solutions for CD experiments.

2.3.2 Fluorescence of Tryptophan in BSA

Fluorescence characterization of BSA was performed on a Horiba Scientific FlurorMax-4 spectrofluorometer (Kyoto, Japan) equipped with a Quantum Northwest Temperature Control Turret (Liberty Lake, WA) and Koolance EXT-440 Liquid Cooling System (Auburn,WA) monitoring the fluorescence of the tryptophan residues with excitation at 285 nm and emission scanning from 300 nm to 500 nm (1 nm step size). Slit widths of 1.5 nm were used for both excitation and emission scans. Characterization of BSA denaturation was done using a temperature melt from 10 to 80^{o}C in 1^{o}C increments with two-minute equilibration time. Sorption experiments were performed in triplicate with the plastic secured on the far back-side of a rectangular 10mm Starna Cells quartz cuvette (Atascadero, CA) using a glass insert designed to not interfere in the measurement. Measurements were taken every five-minutes for one hour with temperature held at 20^{o}C. Figure 2.1 represents the experimental setup for the fluorescence characterization. While this is a bulk solution measurement, perturbations of the fluorescence profile will be due to interaction between the plastic and protein.

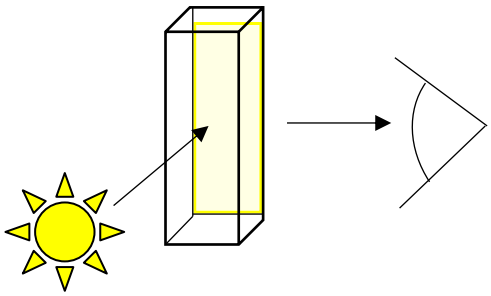

Figure 2.1: Experimental setup for fluorescence characterization. Yellow represents polymer film.

2.3.4 Circular Dichroism of BSA

CD measurements of BSA were performed on an Applied Photophysics Chirascan V100 (Beverly, MA) equipped with a Quantum Northwest TC1 Temperature Control (Liberty Lake, WA) and a S&A CW-3000 Industrial Chiller (Guangzhou, China). Scans of the protein were performed from 250-200 nm (1 nm step size) being held at a constant 20^{o}C in a Hellma 0.5 mm pathlength demountable rectangular quartz cell (Plainview, NY) with the light passing through protein solution then plastic sample. Background scans of PBS buffer were taken, and scans of plastic and buffer were taken to be subtracted from the protein measurements. Scans of protein + plastic combined to monitor changes to protein secondary structure were taken every five minutes after initial exposure for one hour. Because of the role of structural degradation and chemical modifications that occur during polymer degradation, all CD data are reported in m^{o} (acquisition units) to permit comparison between the combined protein-polymer signal and individual polymer CD. Figure 2.2 represents the experimental setup for the CD measurements. Note that orientation of film matters for results as well as ensuring the incident beam goes through the protein solution then the plastic.

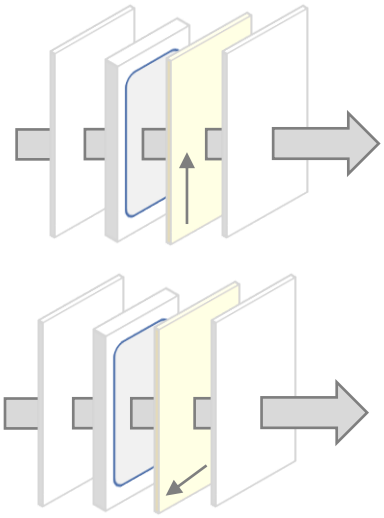

Figure 2.2: Experimental setup for Circular dichroic characterization. Note that orientation of the film (yellow) matters for characterization.

2.4 Data Analysis

2.4.1 Filtering and Processing

Data were analyzed in Matlab (Mathworks, Natick, MA) and post-collection data smoothing was processed using a 2-Gaussian filter via nonlinear least squares fitting algorithm. Fluorescence characterization of the protein sorption onto the plastic of differing irradiation times showed two specific details upon initial observation. The first is that as irradiation time decreased, the fluorescence peak of the tryptophan residues in the protein shifted towards a shorter wavelength emission profile (more details of this shift explored in results and discussion). This can be observed more clearly in Figure 2.3.

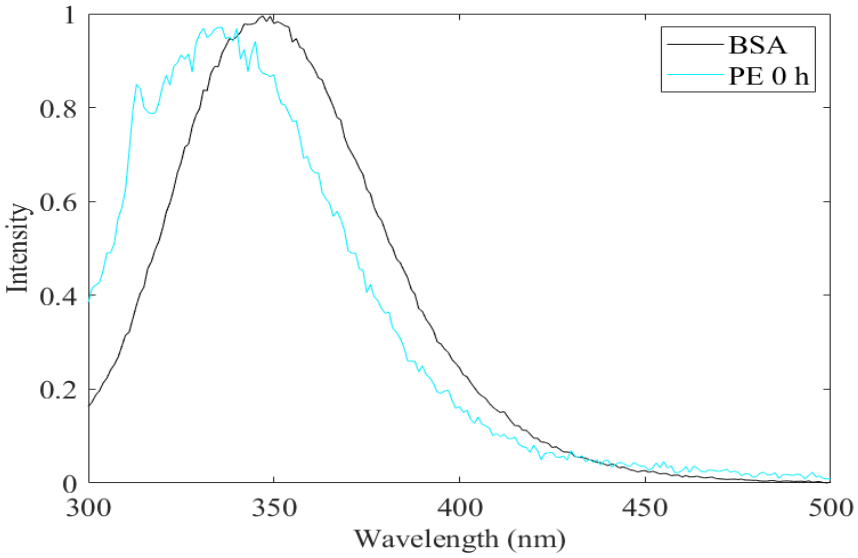

Figure 2.3: Fluorescence spectrum of BSA and BSA exposed to PE 0 hr showing distinct shift in peak upon exposure to a hydrophobic surface. Analyses and fitting were performed from 320-500nm to avoid artifacts at 300-320 nm.

In the PE 0 h, an artifact can be observed in the spectrum at around 315 nm; for this reason, fitting parameters were used for wavelengths 320-500 rather than the full 300-500 spectrum as to avoid any interference of the artifact in the fitting of the data. For filtering, a two-gaussian model fit was used as a post processing data filter rather than others such as a Saviztky-Golay polynomial filtering. Justification of this choice can be

observed in Figure 2.4 showing the differences in fit for the first time point of fluorescence for PE 0 h exposed to BSA.

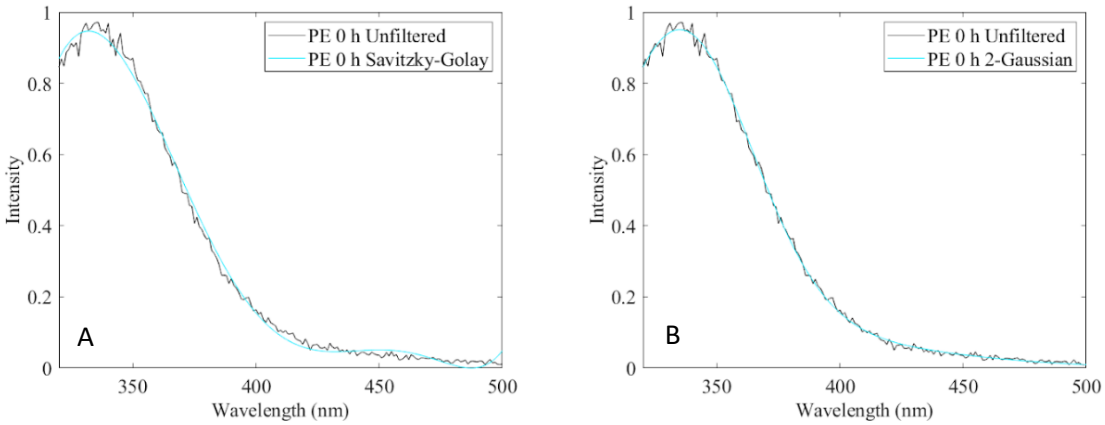

Figure 2.4: Filtering parameters used for post processing noise reduction. Savitzky-Golay filter (A) using a 6th order polynomial fit shows non-existent artifactual peak at 425-475nm as well as a shift in peak max indicating a not good fit. 2-Gaussian fit (B) shows an excellent fit of the data without generation of artificial peaks.

For the filtering using a Saviztky-Golay (SG) filter (Figure 2.2A), a sixth order polynomial equation was used. There are two noticeable problems of this filter fit. First, the SG fit peak does not match the actual data in terms of both intensity and peak location. In fact, the SG filter appears to accentuate a decrease and shift of the peak that could lead to false conclusions. The second problem is that the SG filter causes the generation of a false peak at 425-475nm. This peak formation is inherent to the SG algorithm, and while adding additional degrees to the polynomial might remove this artifact, it will also cause a loss in data characteristics. Figure 2.2B shows the two-Gaussian model, which does not cause the same problems as SG filter, and therefore, it was chosen for further analysis and fitting of the data.

Chapter 3: Results and Discussion

Fluorescence spectroscopy yields insight on conformational changes to a protein upon adsorption to a surface through monitoring the fluorescence profile of the tryptophan residues is highly influenced by their local environment. Within the model protein BSA, there are two tryptophan residues (Trp-134,Trp-212) that can be monitored. Pymol (Schrödinger Inc., New York, NY) modeling allows us to understand the localized environment of the tryptophan in free BSA. Trp-134 is located on the exterior more highly hydrated surface of the protein (Figure 3.1A, red), and Trp-212 is tucked into the more hydrophobic core of the protein (Figure 3.1A, blue). Depending on changes to their local environment, the tryptophan's fluorescence profile changes where a red shift (signal shift to longer wavelengths, lower energy) is indicative of the tryptophan being in a more hydrophilic environment and blue shift due (signal shift to shorter wavelengths, higher energy) to exposure/burial of the tryptophan to a more hydrophobic environment (Royer, 1995). These fluorescence signal shifts can be utilized to determine structural conformation changes to the protein upon adsorption to a given polymer surface through observations of the trends in maximum emission wavelengths and intensity (Royer, 1995).

Figure 3.1A shows the location of each tryptophan and their associated location on their respective alpha-helix. Trp-134 (red) is closer to the exterior of the protein but is surrounded by hydrophobic residues (Figure 3.1A green) and buried in a hydrophobic pocket indicating a less polarized environment (Figure 3.1B). Trp-212 (blue) is located toward the interior of the protein in a solvent accessible cavity and comparatively more polarized environment than Trp-134. Finally, several exposed turns (residues 12-14, 204-

207, 318-322, 394-397, 555-558) have notable hydrophobic content that may contribute to binding and structural rearrangement of the protein on variably charged surfaces.

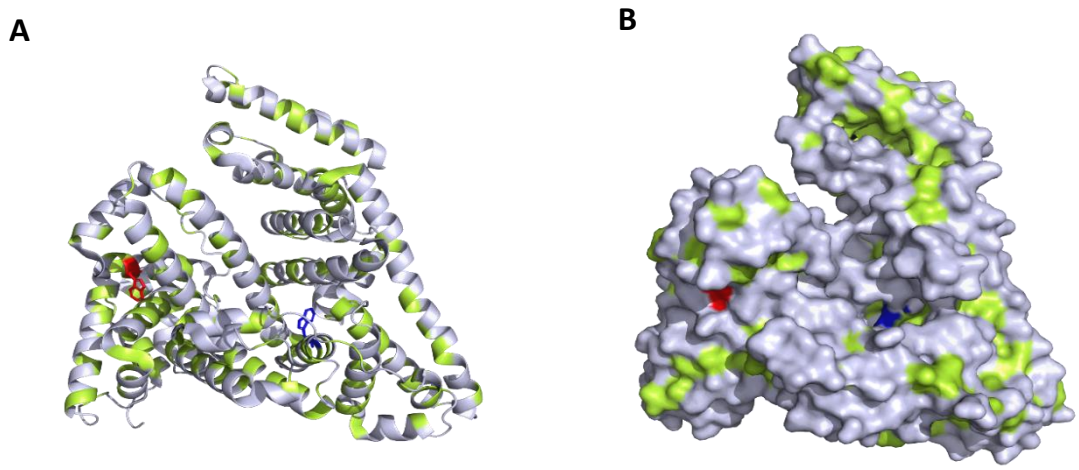

Figure 3.1 A: Pymol projection of PDB file 3V03 (Majorek et al., 2012) BSA cartoon with W134 represented as sticks and highlighted in red and W212 represented by sticks and highlighted in blue. Hydrophobic residues are highlighted in green. **B:** Pymol projection of PDB file 3V03 (Majorek et al., 2012) BSA surface demonstrating solvent accessibility of each tryptophan with W134 represented highlighted in red and W212 highlighted in blue. Hydrophobic residues highlighted in yellow.

Due to the polarized environment of Trp-134, blue shifting in the fluorescence is likely attributed to repacking and minimized solvent accessibility of this residue. This repacking will enhance the hydrophobicity of the surrounding environment. Loss in fluorescence signal may be likely attributed to unhinging of residues 294-306 (Figure 3.2, magenta), responsible for connecting the hemispheres of BSA, that conveniently protect access to Trp-212 (blue). Structural rearrangement in this region causing opening of the structure would be represented by red-shifting or loss of fluorescence signal due to hydration of the tryptophan residue.

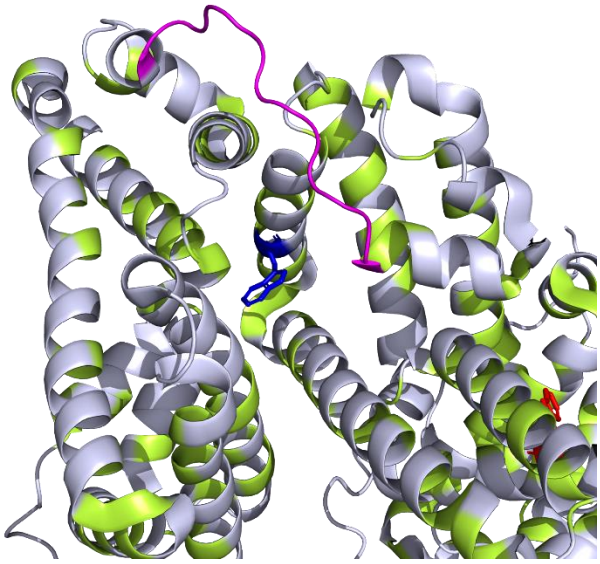

Figure 3.2: Pymol projection of PDB file 3V03 (Majorek et al., 2012) BSA cartoon with W134 represented as sticks and highlighted in red and W212 represented by sticks and highlighted in blue. Hydrophobic residues are highlighted in yellow. Linker residues highlighted in magenta.

3.1 Fluorescence

3.1.1 W-Fluorescence signal variably decreases over the duration of exposure to irradiated PE.

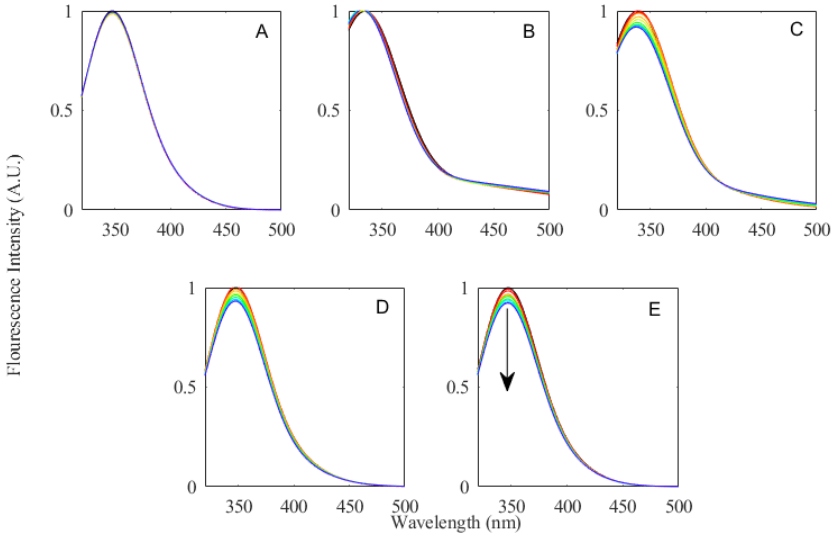

Figure 3.3 : Fluorescence spectra of BSA in PBS exposed to BSA in solution (A), PE 0 h (B), PE 12 h (C), PE 24 h (D), PE 48 h (E) all exposed for 55 minutes with measurements taken every five minutes. Signals were taken in triplicate and normalized to the peak intensity for the initial time point to show trends over time. Scan time represented by black (0 min) to red (55 min).

Figure 3.3 shows the fluorescent trends associated with BSA after exposure to PE at differing stages of photodegradation with the 0 min time point represented in black and all other spectral signals shifting from red to blue over time. For reference, Figure 3.3A shows BSA in free solution monitored over time.

BSA exposure to PE 0 h (Figure 3.3B) demonstrates a peak blue shift to shorter wavelengths by approximately 3 nm with no apparent signal loss over exposure duration.

BSA Trp-fluorescence signal decreases temporally as well as shows a slight blue shift in the peak maximum on exposure to PE 12 h (Figure 3.3C). PE 24 h and PE 48 h (Figure 3.3D and E, respectively) show a temporal loss in fluorescence intensity with no appreciable shift in the fluorescence peak to higher energy (shorter wavelength).

Regardless of the state of degradation of the polymer being exposed to BSA, there is an observable change in the fluorescence profile compared to that of BSA in free solution (Figure 3.3A). This indicates that exposure to the polymer causes changes to the local environment of the tryptophan residues in BSA upon adsorption likely due to structural rearrangement.

3.1.2 Trp-Fluorescence signal blue shift upon exposure to irradiate PE indicates hydrophobic burial.

To better appreciate the significance of the signal shift, the fluorescence peak location was tracked over protein exposure time (Figure 3.4).

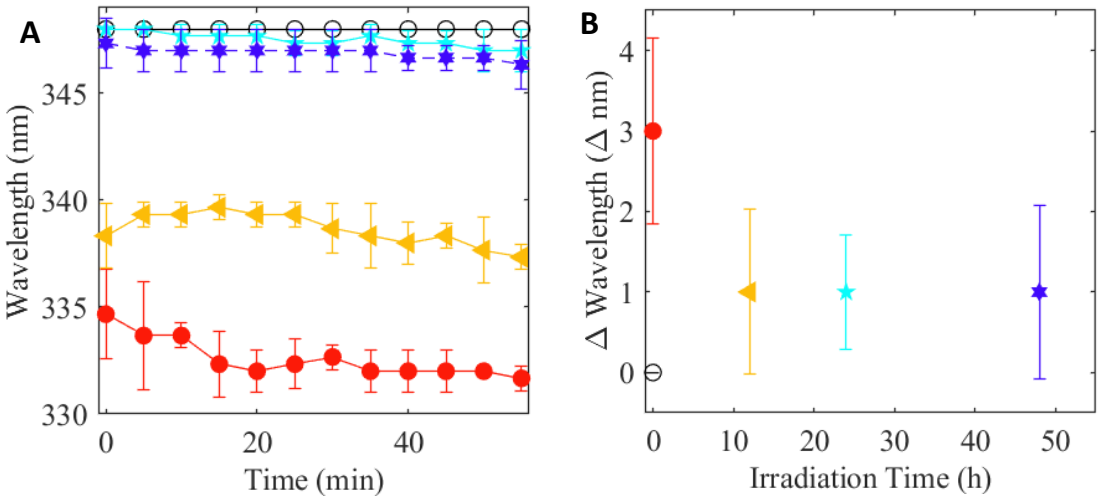

Figure 3.4 A: Temporal fluorescence peak location tracking of free BSA in solution (black circle), PE 0 h (red circle), PE 12 h (yellow triangle), PE 24 h (cyan pentagon), PE 48 h (blue hexagon) in PBS buffer. Error bars represent standard deviation of triplicate measurements. **B:** Change in temporal fluorescence peak location tracking of the duration of exposure overlay of free BSA in solution (black circle), PE 0 h (red circle), PE 12 h (yellow triangle), PE 24 h (cyan pentagon), PE 48 h (blue hexagon) in PBS buffer. Error bars represent standard deviation of triplicate measurements.

Figure 3.4A shows the shift in fluorescence peak location over time of BSA with exposure to polyethylene at various degrees of photodegradation. BSA signal (black circle) shows no change to fluorescence peak location over 55 min. PE 0 h and PE 12 h (red circles and yellow triangles) show an initial peak location 12 nm and 10 nm lower than the signal from free BSA in solution indicative of hydrophobic burial of the tryptophan upon initial interaction with unaged and minimally aged polymer surfaces. The dramatic shift, even at the initial fluorescence measurement may point to the protein initially docking on a time scale faster than our testing parameters (Figure 3.4A). Peaks for PE 0 h and PE 12 h continue to blue shift over exposure time (3 nm and 1 nm)

demonstrating a protein repacking into a more hydrophobic environment (Figure 3.4B). PE 24 h and PE 48 h (cyan pentagons and blue hexagons) initially have a fluorescence peak location 0 nm and 1 nm lower than that of non-PE exposed BSA (Figure 3.4B). Peaks for PE 24 h and PE 48 h have minimal temporal shift (1 nm) indicating no protein rearrangement that alters the local environment of the tryptophan residues (Figure 3.4B).

Fluorescence peak shifts suggest photo-induced hydrophobicity changes to the polymer play a dominant role in the protein-polymer interaction. The shift in fluorescence maximum relates to the extent of photodegradation, where a more dramatic blue shift is observed with decreasing photodegradation. That is, unaged PE, the most hydrophobic PE surface, has the most dramatic effect on the fluorescence peak signal whereas PE 48 h (i.e., the most hydrophilic surface) has the least effect on fluorescence signal shift. Additionally, the temporal shift in fluorescence maximum is greatest with decreasing photodegradation. This is indicative of the burial of the tryptophan residue into the hydrophobic core of the protein or a loss in the polarized environment due to dehydration of the surface shell upon binding (Pabbathi et al., 2013; L. Zhang et al., 2015). For example, Geng et al., exposed BSA to a long-chain (hydrophobic) imidazolium ionic liquid that denatured BSA. This caused the intrinsic fluorophore (Trp) to bury itself in a local hydrophobic microenvironment shown through fluorescence blue shifting (Geng et al., 2010). Ghosh et al. showed binding of a charge transfer fluoroprobe (MMAPA) that specifically bound to less polar, hydrophobic, restricted environments led to significant blue shifting again indicating that in hydrophobic environments the peak maxima will blue shift (Ghosh et al., 2012). It is well documented that PE photo-oxidizes, yielding a more hydrophilic polymer surface with longer irradiation time (Hebner &

Maurer-Jones, 2020; Maurer-Jones & Monzo, 2021). Characterizing our polymer films with ATR-FTIR, we similarly observe an increase in hydrophilicity with time as shown in Figure 3.5, where the carbonyl index increases with irradiation time.

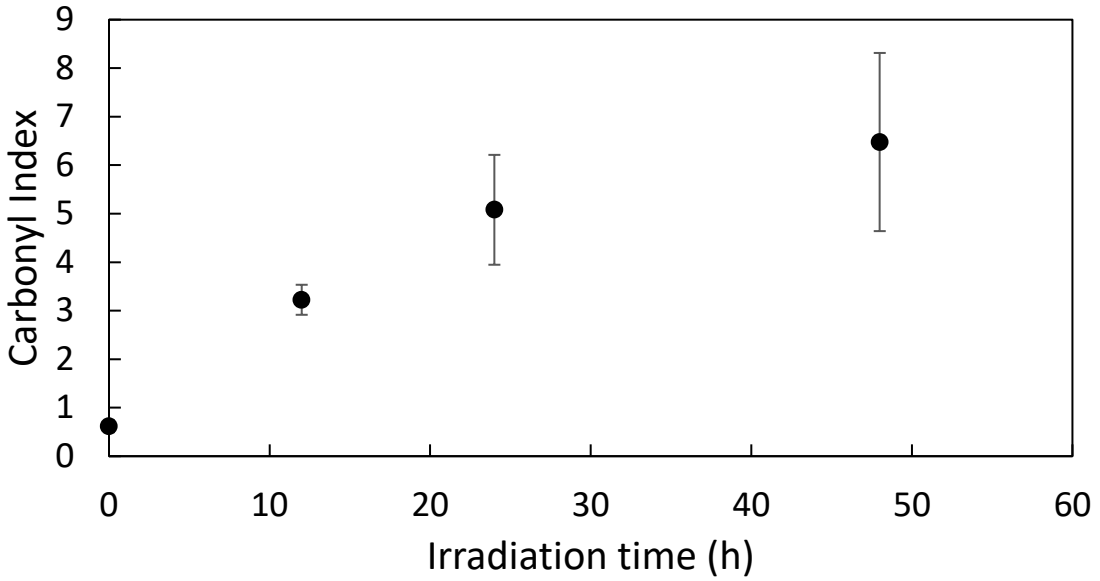

Figure 3.5: Carbonyl index values for PE at various stages of photoirradiation. Markers represent averages of triplicate spectra taken at different location on the film plus or minus the standard deviation.

The trend in fluorescence peak location follows that of hydrophilicity of the surface (caused by increase in carbonyl index), where increasing the hydrophilicity of the surface causes less shifts in the fluorescence wavelength maximum (Figure 3.4A). Interestingly, PE 24 and 48 h irradiation cause a minimal shift in the peak location of the fluorescence (Figure 3.4B), which may indicate that once the polymer surface reaches a threshold hydrophilicity, further photo-oxidation does not impact what hydrophilicity the BSA experiences. One notable difference between the BSA fluorescence in the presence of these extensively photodegraded polymers compared to no PE, however, is that there still remains a slight blue shift in the fluorescence peak location over time (Figure 3.4B)

indicating the potential for some structural rearrangement on the surface although it is much slower than that for exposure to polymers that are less photodegraded.

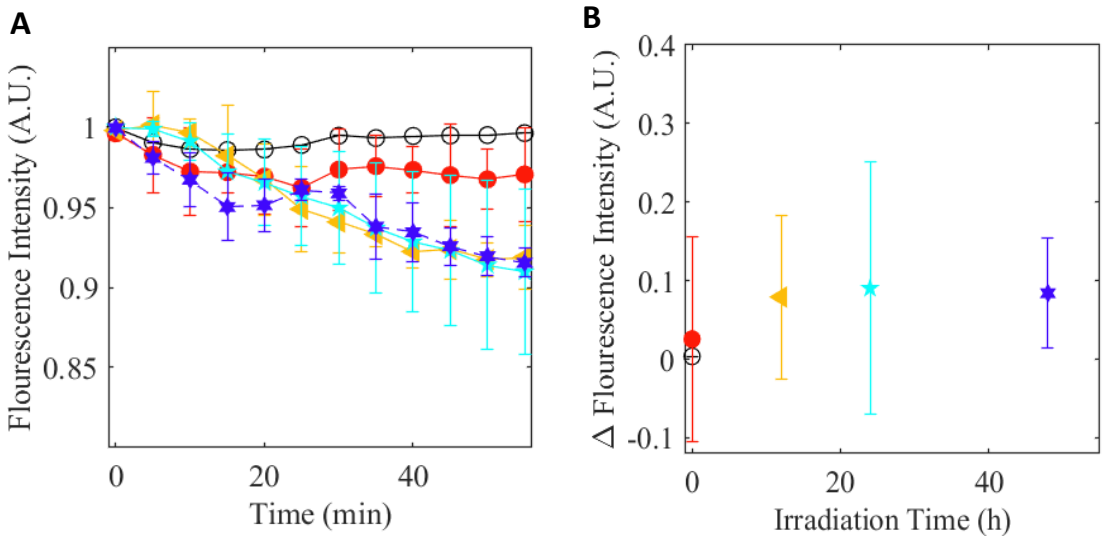

Figure 3.6A: Temporal fluorescence peak maximum tracking overlay of free BSA in solution (black circle), PE 0 h (red circle), PE 12 h (yellow triangle), PE 24 h (cyan pentagon), PE 48 h (blue hexagon) in PBS buffer. Error bars represent standard deviation of triplicate measurements. **B:** Change in temporal fluorescence peak maximum tracking over the duration of exposure (0 min - 55 min) overlay of free BSA in solution (black circle), PE 0 h (red circle), PE 12 h (yellow triangle), PE 24 h (cyan pentagon), PE 48 h (blue hexagon) in PBS buffer. Error bars represent standard deviation of triplicate measurements.

We also observed variable decreases in the fluorescence intensity upon exposure to photodegraded PE. Figure 3.6A shows the normalized fluorescence max over time with exposure to variously aged PE. Excluding PE 0 h, with exposure to PE there is a temporal decrease in the peak fluorescence intensity. Figure 3.6B demonstrates a possible trend between film aging and decrease in fluorescence intensity, where film aging results in an increased loss of fluorescence over time. Interestingly, unaged PE (red circle) has the strongest initial peak location shift (Figure 3.4A) and largest peak shift over time (Figure 3.4B) and the least intensity loss suggesting that the protein initially interacts with the hydrophobic polymer surface and undergoes rearrangement with no significant

opening of the protein (Figure 3.6A and B). The BSA exposed PE 48 h shows initial docking onto an aged, hydrophilic surface with minimal initial structural perturbation. The decrease in PE 48 h fluorescence demonstrates that the protein most likely unfolds or rearranges along the hinge region of the protein (Figure 3.2, magenta) over the duration of polymer exposure resulting in hydration of the Trp-212 yielding a decrease in fluorescence intensity. This is likely due to the addition of exposed charged functional groups of the protein interacting with the carbonyl-enriched surface of the irradiated plastic. This causes changes in the tryptophan's local micro-environment initiating fluorescence quenching due to hydration.

3.2 Circular Dichroism

While fluorescence allows us to understand and probe the local environment of the tryptophan residues and its polarity upon restructuring on the surface of the polymer, we can further interrogate and identify secondary structural changes through polarized light techniques such as CD. CD provides information regarding the secondary structural characteristics of a protein through changes in differential adsorption of polarized light. BSA's highly helical nature can be easily recognized through CD by the characteristic differential absorbance of left-circularly polarized light minus right circularly polarized light that results in two reported troughs at 208 and 222 nm. Monitoring changes to this spectrum over time can help elucidate how the helical composition of the protein changes upon adsorption to the polymer.

3.2.1 Intrinsic CD Signal Comparison of BSA Exposed to Irradiated PE Show Change in Initial Structural Variation.

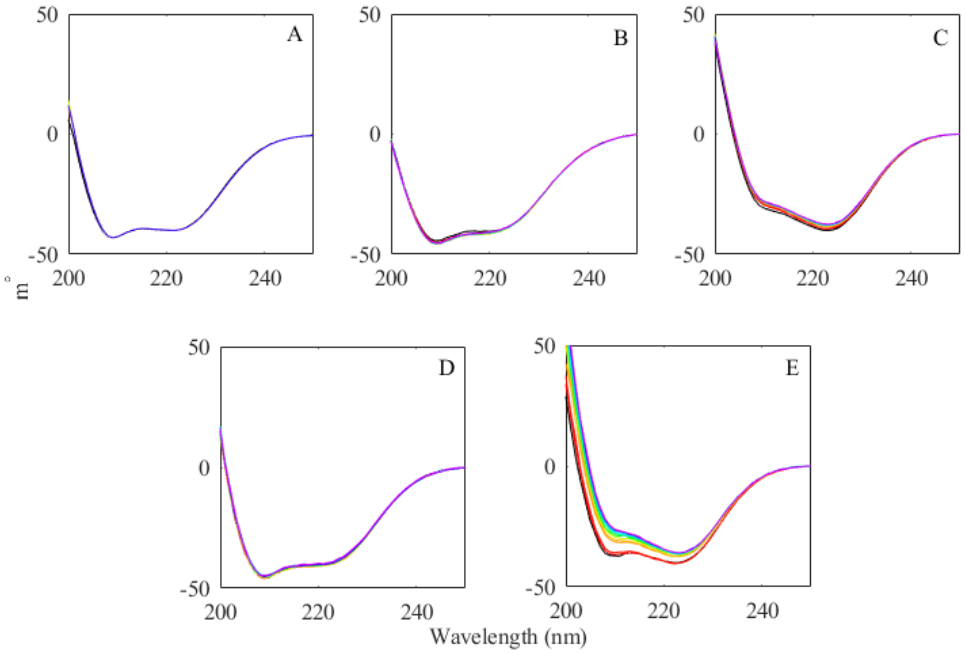

Figure 3.7 Intrinsic CD spectra averaged over triplicate measurements of (A) BSA in solution, (B) BSA exposed to 0 h irradiated PE over 55 minutes, (C) BSA exposed to 12 h irradiated PE over 55 minutes, (D) BSA exposed to 24 h irradiated PE over 55 minutes, and (E) BSA exposed to 48 h irradiated PE over 55 minutes. All signals were normalized to 0 at 250 nm to account for minimal variation in protein-polymer interactions between samples. Scan time is represented from black (0 min) to magenta (55 min).

Figure 3.7 shows the averaged CD spectra at each exposure time point of BSA to PE at various stages of photodegradation. Error bars are smaller than the line width for each scan and each sample. Each CD spectrum reflects the signal from both BSA and PE where applicable. Free BSA in solution was investigated over time to provide comparison (Figure 3.7A).

PE 0 h exposed BSA (Figure 3.7B) shows minimal signal change over time of exposure demonstrating that protein absorption to unaged polymer surface does not result in structural rearrangement of the protein. A noticeable signal change at approximately

215 nm may be the result of loss of in helical content. The 208 nm signal is comparatively stronger (more negative) than the 222 nm alpha helical signal suggesting a tightened alpha helical conformation compared to free BSA. This helical tightening can be validated by the blue shifting, more hydrophobic tryptophan environment (i.e., fluorescence signal observation of Figure 3.3B and Figure 3.4), and spectral shift in both the CD and the fluorescence would be expected for protein rearrangement upon binding to the hydrophobic polymer surface. These findings further support that during structural rearrangement upon adsorption to the polymer, that the tryptophan residues undergo potential hydrophobic burial resulting in further signal blue shifting. These findings in coordination with minimal protein unfolding as seen in the CD may point to the protein opening along the hinge region (Figure 3.2, magenta) further burying Trp-212 into a hydrophobic pocket with turn rearrangement to accommodate this interaction.

PE 12 h (Figure 3.7 C) shows a definitive loss of helical structure via the general loss in ellipticity between 205-230 nm over time. The signal at 208 nm is higher than that at 222 nm indicating tightening of the helical structure. The definitive loss in ellipticity of the exposure, paired with the loss in fluorescence signal (Figure 3.6), indicates that there is large structural rearrangement and that the structure seems to be rearranging to bury the tryptophan residues into a more hydrophobic environment.

PE 24 h (Figure 3.7D) exhibit the same BSA initial secondary structural signal seen with PE 0 h exposure and minimal signal loss over exposure time representative of some loss in helicity. PE 24 h fluorescence shows minimal peak shift deviation from free BSA (Figure 3.3D and Figure 3.4) as well as less peak movement over the duration of polymer exposure suggesting that protein binding is to a more hydrophilic surface. In

combination with the minimal fluorescence wavelength signal maxima shift, the CD data suggests the protein binds, but rearrangement is attenuated. This indicates that the protein unfolds to a small degree in comparison to samples at photochemical transformation transition points.

PE 48 h (Figure 3.7E) exhibits a markedly different initial intrinsic signal in comparison to PE 0 h and PE 24 h. The PE 48 h signal shows structural similarities to the BSA exposed to PE 12 h, specifically, a deeper trough around 222 nm and lessening of the trough at 208 nm. The PE 48 h exposed BSA demonstrates the most pronounced signal loss over time, resulting in a dramatic shift upward around 208 nm. The replicability of the spectra suggests a real time correlation generating large spacing gaps between the earlier (red) and later (blue) spectra. This spacing is most pronounced between 222 nm and 205 nm. Tryptophan fluorescence (Figure 3.3E, Figure 3.4) shows less signal response to polymer exposure suggesting that the structural changes during protein absorption and unfolding do not dramatically affect the local environment of the tryptophan. Further, the initial peak location of the BSA in fluorescence suggests the protein initially binds to a relatively hydrophilic environment. Interestingly, the PE 48 h sample shows the largest overall peak signal loss (Figure 3.6) as well as minimal peak location blue shifting (Figure 3.4) indicative of minimal environmental change around either tryptophan. Both tryptophan's are located mid-helix (Figures 3.1, 3.2, blue and red sticks). Any structural rearrangement in the region of the amino acid would result in a shift or signal loss in the fluorescence. Because the fluorescence shows no evidence of major structural rearrangement causing a change to the local environments of the tryptophan residues, the CD signal reflects the protein accommodating a tighter

conformation upon binding with helical tightening at the edges of helices and turn regions.

3.2.2 Total 222 nm CD signal shows BSA alpha helical content loss over exposure time enhanced as PE ages.

To better elucidate the specifics of the changes to the structure upon adsorption, the individual wavelength 208nm, 215nm and 222nm, mentioned previously, were plotted in Figure 3.8.

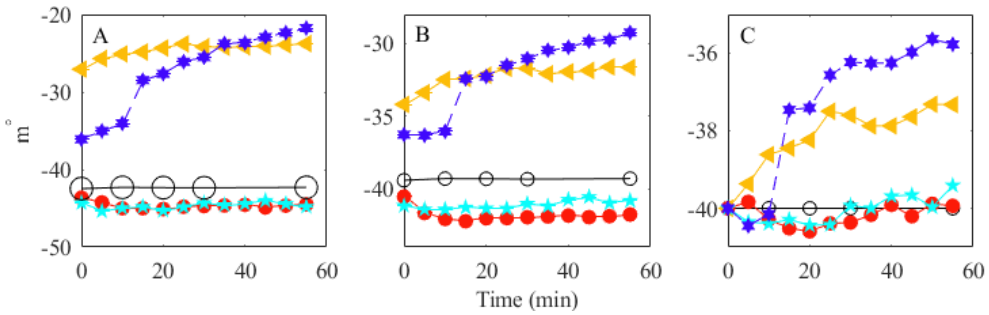

Figure 3.8 A: Averaged 208 nm total CD signal overlay of 7.5 μM BSA with 0h (red circle), 12 h (yellow triangle), 24 h (cyan pentagon), 48 h (blue hexagon) PE films in PBS buffer. **B:** Averaged 215 nm total CD signal overlay of 7.5 μM BSA with 0h (red circle), 12 h (yellow triangle), 24 h (cyan pentagon), 48 h (blue hexagon) PE films in PBS buffer. **C:** Averaged 222 nm total CD signal overlay of 7.5 μM BSA with 0h (red circle), 12 h (yellow triangle), 24 h (cyan pentagon), 48 h (blue hexagon) PE films in PBS buffer. Error bars are smaller than all data points in figure.

Figure 3.8A compares 208 nm CD signal (pi→pi*transition for helical structures) from the subtracted BSA-polymer exposure for each aged polymer sample. PE 24 h shows the same minimal signal change over time as the PE 0 h exposure. PE 12 h and 48 h aged samples show a smaller initial ellipticity. PE 12 h reports some signal loss but only PE 48 h clearly demonstrates a pronounced (~13 elliptical units) signal loss over the time of polymer exposure (Figure 3.8A).

Figure 3.8B reports the 215 nm signal over the sample duration of polymer exposure, the saddle point for helical signature. Specifically, 215 nm corresponds to both

$pi \rightarrow pi^*$ and $n \rightarrow pi^*$ of beta sheets but will also demonstrate linear signal loss if helical structures are converted to random coils. PE 0 h sample decreases slightly over the sampling time while all other samples increase suggesting PE 0 h may undergo some structural rearrangement that varies from all other samples. PE 24 h has the same approximate elliptical signal as PE 0 h in comparison to other aged samples but does not follow the same PE 0 h trend. PE 12 h signal shows a slight loss in ellipticity over time and PE 48 h sample shows a dramatic decrease in ellipticity in comparison to other aged samples (~7 elliptical units). Signal loss at 215 nm could be attributed to a loss of alpha helical composition, alpha helical unraveling or a gain in turn sequence as Beta sheet formation in BSA is highly unlikely due to its extensively helical (and turn-containing) structure (Figures 3.1 and 3.2).

Figure 3.8C tracks the 222 nm total CD signal for BSA and each irradiated polymer over a 55-minute period. BSA exposed to PE 0 h (red circle) and PE 24 h (pentagon) show no appreciable temporal loss in ellipticity. PE 12 h demonstrates a stronger initial signal loss over this initial 15-minute exposure period; however, the signal loss persists more dramatically with fluctuations for the duration of sampling. PE 48 h shows a (2 elliptical unit) signal loss between the 10- and 15-minute time points with a temporal trend similar to that of PE 12 h exposure.

3.2.3 222 nm - 208 nm difference CD signals demonstrate protein unfolding and structural rearrangement.

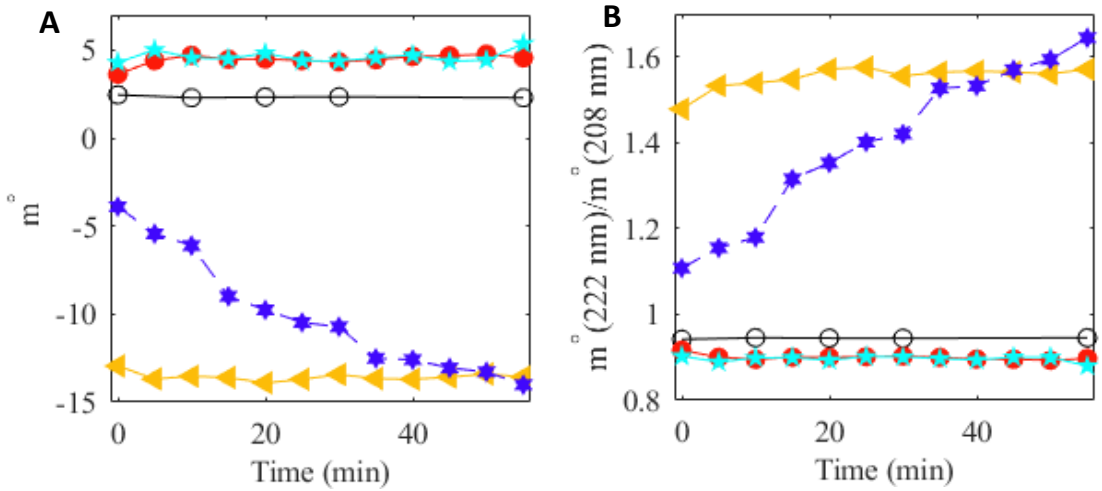

Figure 3.9A: Averaged 222-208 nm total CD signal overlay of 7.5 μM BSA exposed to 0h (red circle), 12 h (yellow triangle), 24 h (cyan pentagon), 48 h (blue hexagon) PE films in PBS buffer. Error bars are smaller than all data points in figure. **B :** 222/208 nm alpha helical ratio total CD signal overlay of 7.5 μM BSA with 0h (red circle), 12 h (yellow triangle), 24 h (cyan pentagon), 48 h (blue hexagon) PE films in PBS buffer. Error bars are smaller than all data points in figure.

Figure 3.9A PE irradiated for 0 h, 12 h, and 24 h show no variational signal loss between the 208 nm and 222 nm peaks over the duration of polymer exposure. Any resultant loss in ellipticity is due to protein unfolding for these samples. PE 48 h shows an enhanced difference in ellipticity between 208 nm and 222 nm suggesting an unequal loss of signal more indicative of a helical rearrangement to a more constrained helical structure. The corresponding fluorescence signal intensity (Figure 3.6A) decreases over time for 48 h with no apparent peak shift (Figure 3.4A). The protein likely initially docks on the hydrophilic polymer surface using polar surface residues and then rearranges to accommodate a more preferential orientation for hydrophobic turn regions by tightening the ends of adjacent alpha helical regions. The lack of blue shifting (Figure 3.4A)

suggests that the local environment around Trp-134 (Figure 3.1A) is not perturbed. The decrease in fluorescence intensity (Figure 3.5A) most likely corresponds to Trp-212 surface induced quenching as there is no red-shifting that would be present from hydration.

222nm/208nm CD ratio (Figure 3.9B) supports the helical tightening during rearrangement of the BSA 48 h PE sample (blue hexagon). A 222 nm/208nm ratio exceeding 1.2 is indicative of the more constrained 3.10 alpha helical secondary structure. PE 0 h and 24 h show no increase above the alpha helical transition ratio (1.2) corroborating CD signal evidence (figures 3.9 A and B) that BSA unfolds on these surfaces with no obvious structural rearrangement (Creighton, 2010). While PE 12 h does exhibit a 222nm/208nm difference and ratio that lies closer to 48 h, it does not dramatically change over the time-course of measurement. We concluded that this captures and entropically favored state; yet it doesn't show changes over time that we'd expect with tightening that was clearly demonstrated with the most photodegraded polymer.

3.4 Comparing polymer characteristics to BSA binding yields insight into structural rearrangement.

Increases to the polymers hydrophilicity due to incorporation of carbonyl groups results in an increase in associated surface area. However, the atomic level surface area of polymers shows limited perturbation to protein absorption. Therefore, chemical changes due to irradiation at the interface of the polymer drive protein adsorption behavior (Han et al., 2003). These chemical changes from irradiation show an increase in carbonyl content (Figure 3.5). However, bulk crystallinity measurements show an initial increase at PE 12 h, a plateau until PE 24 h, and finally another increase at PE 48 h (Figure 3.10).

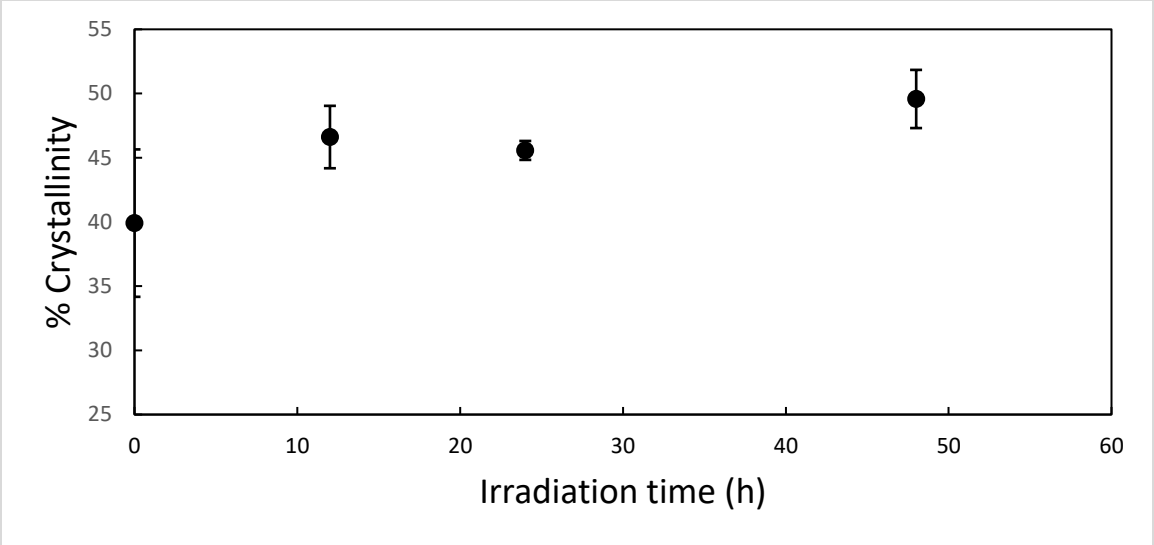

Figure 3.10: First melt DSC bulk crystallinity measurements of photodegraded PE. Error bars represent the plus or minus the standard deviation of triplicate measurements.

Observations into the trends in crystallinity show that there is minimal differences between irradiation points. However, there is the largest temporal change to the helical character of BSA upon adsorption to PE 48 h (Figure 3.9). At this time point we begin to see an increase in the bulk crystallinity as well as the highest carbonyl content indicating that these structural changes alter the way BSA adsorbs to the surface.

Observing the trends in the fluorescence wavelength maximum (Figure 3.4) upon exposure to PE 48 h shows little perturbation to the local environment of the tryptophan residues. This shows that the changes to the helical structures do not interfere with the structural characteristics of the protein around these residues. The tryptophans in BSA are located towards the center of the helical structure (Figure 3.1 and 3.2), and minimal perturbation to their environment upon adsorption indicates that the helices are likely tightening towards the edges and not the middle. These structural changes are not stable under natural conditions and indicate that the protein's structure is being stabilized by the carbonyl groups on the surface of the irradiated polymer upon adsorption. This

stabilization shows the relationship between an increase in carbonyl index (i.e., increase in hydrophilicity) and changes to structural characteristics causing an increase in the strength of protein binding.

Chapter 4 : Conclusions

Through this work we confirmed that an increase in carbonyl index (i.e., increase in hydrophilicity) yields a smaller perturbation to the local environment of the tryptophan residues upon adsorption to PE. This is observable by smaller shifts in the fluorescence wavelength maximum upon exposure to more highly photodegraded polymers. We also demonstrated, through trends in CD, that there was an increase in structural rearrangement of BSA upon exposure to both PE 12 and 48 h. However, there was minimal temporal change to the CD signal with exposure to PE 12 h likely indicating that we missed the initial binding phenomena (Figure 3.9). The greatest temporal change to the CD signal occurred upon exposure to PE 48 h. These structural changes are not stable naturally and were therefore stabilized by the carbonyl groups on the surface of irradiated polymers. This indicates that an increase in the photodegradation of PE will result in an increase in binding strength of proteins onto its surface.

These results show that there is a distinct trend between the degradation of plastic and their interactions with microbial species. This helps to further understand this relationship between the abiotic and biotic degradation pathways of the plastics after they enter our environment. Understanding this relationship more fully will help in generating methods to deal with the plastic waste that is currently in our environment as well as potentially helping in the design of plastic that is more readily degraded.

Bibliography

Allen, N. S., & McKellar, J. F. (1975). Photodegradation and stabilization of commercial polyolefins. *Chemical Society Reviews*, *4*(4), 533–547. https://doi.org/10.1039/CS9750400533

Amaral-Zettler, L. A., Zettler, E. R., & Mincer, T. J. (2020). Ecology of the plastisphere. *Nature Reviews Microbiology*, *18*(3), 139–151. https://doi.org/10.1038/s41579-019-0308-0

Amelia, T. S. M., Khalik, W. M. A. W. M., Ong, M. C., Shao, Y. T., Pan, H. J., & Bhubalan, K. (2021). Marine microplastics as vectors of major ocean pollutants and its hazards to the marine ecosystem and humans. *Progress in Earth and Planetary Science*, *8*(1). https://doi.org/10.1186/s40645-020-00405-4

Ansyln, E., & Dougherty, D. (2006). *Modern Physical Organic Chemistry*.

Berne, C., Ducret, A., Hardy, G. G., & Brun, Y. V. (2015). Adhesins Involved in Attachment to Abiotic Surfaces by Gram-Negative Bacteria. *Microbial Biofilms*, *3*(4), 163–199. https://doi.org/10.1128/9781555817466.ch9

Berova, N., Polavarapu, P., Nakanishi, K., & Woody, R. (2012). *Comprehensive Chiroptical Spectroscopy Vol. 2* (John Wiley and Sons (ed.)). Wiley.

Blaine, R. (n.d.). Polymer Heats of Fusion. *TA*.

Cavalli, A., Salvatella, X., Dobson, C. M., & Vendruscolo, M. (2007). Protein structure determination from NMR chemical shifts. *Proceedings of the National Academy of Sciences of the United States of America*, *104*(23), 9615–9620. https://doi.org/10.1073/pnas.0610313104

Chamas, A., Moon, H., Zheng, J., Qiu, Y., Tabassum, T., Jang, J. H., Abu-Omar, M., Scott, S. L., & Suh, S. (2020). Degradation Rates of Plastics in the Environment. *ACS Sustainable*

Chemistry and Engineering, *8*(9), 3494–3511. https://doi.org/10.1021/acssuschemeng.9b06635

Cooley, R., Arp, D., & Karplus, A. (2010). Evolutionary origin of a secondary structure: π-helices as cryptic but widespread insertional variations of α-helices enhancing protein functionality. *Molecular Biology*, *404*(2), 232–246. https://doi.org/10.1016/j.jmb.2010.09.034.Evolutionary

Creighton, T. (2010). *The Biophysical Chemistry of Nucleic Acids and Proteins*. Helvetian Press.

Deller, M. C., Kong, L., & Rupp, B. (2016). Protein stability: A crystallographer's perspective. *Acta Crystallographica Section:F Structural Biology Communications*, *72*, 72–95. https://doi.org/10.1107/S2053230X15024619

Donlan, R. M., & Costerton, J. W. (2002). Biofilms: Survival mechanisms of clinically relevant microorganisms. *Clinical Microbiology Reviews*, *15*(2), 167–193. https://doi.org/10.1128/CMR.15.2.167-193.2002

Eisenberg, D. (2003). The discovery of the α-helix and β-sheet, the principal structural features of proteins. In *Proceedings of the National Academy of Sciences of the United States of America* (Vol. 100, Issue 20, pp. 11207–11210). https://doi.org/10.1073/pnas.2034522100

F2102-17, A. (n.d.). *Standard Guid for Evaluationg the Extent of Oxidation in Polyethylene Fabricated Forms Intended for Surgical Implants*. https://doi.org/10.1520/F2102-17

Felgueiras, H. P., Antunes, J. C., Martins, M. C. L., & Barbosa, M. A. (2018). Fundamentals of protein and cell interactions in biomaterials. In *Peptides and Proteins as Biomaterials for Tissue Regeneration and Repair*. Elsevier Ltd. https://doi.org/10.1016/B978-0-08-100803-4.00001-2

Gao, J., Lu, Y., Wei, G., Zhang, X., Liu, Y., & Qiao, J. (2002). Effect of radiation on the

crosslinking and branching of polypropylene. *Journal of Applied Polymer Science*, *85*(8), 1758–1764. https://doi.org/10.1002/app.10716

Gardette, M., Perthue, A., Gardette, J. L., Janecska, T., Földes, E., Pukánszky, B., & Therias, S. (2013). Photo- and thermal-oxidation of polyethylene: Comparison of mechanisms and influence of unsaturation content. *Polymer Degradation and Stability*, *98*(11), 2383–2390. https://doi.org/10.1016/j.polymdegradstab.2013.07.017

Gauto, D. F., Estrozi, L. F., Schwieters, C. D., Effantin, G., Macek, P., Sounier, R., Sivertsen, A. C., Schmidt, E., Kerfah, R., Mas, G., Colletier, J. P., Güntert, P., Favier, A., Schoehn, G., Schanda, P., & Boisbouvier, J. (2019). Integrated NMR and cryo-EM atomic-resolution structure determination of a half-megadalton enzyme complex. *Nature Communications*, *10*(1), 1–12. https://doi.org/10.1038/s41467-019-10490-9

Geng, F., Zheng, L., Yu, L., Li, G., & Tung, C. (2010). Interaction of bovine serum albumin and long-chain imidazolium ionic liquid measured by fluorescence spectra and surface tension. *Process Biochemistry*, *45*(3), 306–311. https://doi.org/10.1016/j.procbio.2009.10.001

Gewert, B., Plassmann, M. M., & Macleod, M. (2015). Pathways for degradation of plastic polymers floating in the marine environment. *Environmental Sciences: Processes and Impacts*, *17*(9), 1513–1521. https://doi.org/10.1039/c5em00207a

Geyer, R., Jambeck, J. R., & Law, K. L. (2017). Production, use, and fate of all plastics ever made. *Science Advances*, *3*(7), 25–29. https://doi.org/10.1126/sciadv.1700782

Ghosh, S., Jana, S., & Guchhait, N. (2012). Domain specific association of small fluorescent probe trans -3-(4-monomethylaminophenyl)-acrylonitrile (MMAPA) with bovine serum albumin (BSA) and its dissociation from protein binding sites by Ag nanoparticles: Spectroscopic and molecular docking study. *Journal of Physical Chemistry B*, *116*(3), 1155–1163. https://doi.org/10.1021/jp2094752

Goodfellow. (n.d.). *Polyethylene - Low Density(LDPE) - Film -Material Information*. http://www.goodfellow.com/A/Polyethylene-Low-Density-Film.html

Han, M., Sethuraman, A., Kane, R. S., & Belfort, G. (2003). Nanometer-scale roughness having little effect on the amount or structure of adsorbed protein. *Langmuir*, *19*(23), 9868–9872. https://doi.org/10.1021/la030132g

Hebner, T. S., & Maurer-Jones, M. A. (2020). Characterizing microplastic size and morphology of photodegraded polymers placed in simulated moving water conditions. *Environmental Science: Processes and Impacts*, *22*(2), 398–407. https://doi.org/10.1039/c9em00475k

Hermabessiere, L., Dehaut, A., Paul-Pont, I., Lacroix, C., Jezequel, R., Soudant, P., & Duflos, G. (2017). Occurrence and effects of plastic additives on marine environments and organisms: A review. *Chemosphere*, *182*, 781–793. https://doi.org/10.1016/j.chemosphere.2017.05.096

Hlady, V., & Buijs, J. (1996). Protein adsorption on solid surfaces. *Current Opinion in Biotechnology*, *7*(1), 72–77. https://doi.org/10.1016/S0958-1669(96)80098-X

Hsieh, S. R., Reddy, P. M., Chang, C. J., Kumar, A., Wu, W. C., & Lin, H. Y. (2016). Exploring the behavior of bovine serum albumin in response to changes in the chemical composition of responsive polymers: Experimental and simulation studies. *Polymers*, *8*(6). https://doi.org/10.3390/polym8060238

Issac, M. N., & Kandasubramanian, B. (2021). Effect of microplastics in water and aquatic systems. *Environmental Science and Pollution Research*, *28*(16), 19544–19562. https://doi.org/10.1007/s11356-021-13184-2

Jeyachandran, Y. L., Mielczarski, E., Rai, B., & Mielczarski, J. A. (2009). Quantitative and qualitative evaluation of adsorption/desorption of bovine serum albumin on hydrophilic and hydrophobic surfaces. *Langmuir*, *25*(19), 11614–11620. https://doi.org/10.1021/la901453a

Kaiser, D., Kowalski, N., & Waniek, J. J. (2017). Effects of biofouling on the sinking behavior of microplastics. *Environmental Research Letters*, *12*(12). https://doi.org/10.1088/1748-9326/aa8e8b

Kalasin, S., & Santore, M. M. (2009). Non-specific adhesion on biomaterial surfaces driven by small amounts of protein adsorption. *Colloids and Surfaces B: Biointerfaces*, *73*(2), 229–236. https://doi.org/10.1016/j.colsurfb.2009.05.028

Katsikogianni, M., Missirlis, Y. F., Harris, L., & Douglas, J. (2004). Concise review of mechanisms of bacterial adhesion to biomaterials and of techniques used in estimating bacteria-material interactions. *European Cells and Materials*, *8*, 37–57. https://doi.org/10.22203/eCM.v008a05

Kedzierski, M., D'Almeida, M., Magueresse, A., Le Grand, A., Duval, H., César, G., Sire, O., Bruzaud, S., & Le Tilly, V. (2018). Threat of plastic ageing in marine environment. Adsorption/desorption of micropollutants. *Marine Pollution Bulletin*, *127*(December 2017), 684–694. https://doi.org/10.1016/j.marpolbul.2017.12.059

Krejchi, M. T., Cooper, S. J., Deguchi, Y., Atkins, E. D. T., Fournier, M. J., Mason, T. L., & Tirrell, D. A. (1997). Crystal structures of chain-folded antiparallel β-sheet assemblies from sequence-designed periodic polypeptides. *Macromolecules*, *30*(17), 5012–5024. https://doi.org/10.1021/ma9614050

Kujirai, C., Hashiya, S., Furuno, H., & Terada, N. (1968). Photochemical crosslinking of polypropylene. *Journal of Polymer Science Part A-1: Polymer Chemistry*, *6*(3), 589–593. https://doi.org/10.1002/pol.1968.150060314

Lanyi, F. J., Wenzke, N., Kaschta, J., & Schubert, D. W. (2018). A method to reveal bulk and surface crystallinity of Polypropylene by FTIR spectroscopy - Suitable for fibers and nonwovens. *Polymer Testing*, *71*, 49–55.

https://doi.org/10.1016/j.polymertesting.2018.08.018

Lebaron, R. G., & Athanasiou, K. A. (2000). Extracellular matrix cell adhesion peptides: Functional applications in orthopedic materials. *Tissue Engineering*, *6*(2), 85–103. https://doi.org/10.1089/107632700320720

Lebreton, L., Slat, B., Ferrari, F., Sainte-Rose, B., Aitken, J., Marthouse, R., Hajbane, S., Cunsolo, S., Schwarz, A., Levivier, A., Noble, K., Debeljak, P., Maral, H., Schoeneich-Argent, R., Brambini, R., & Reisser, J. (2018). Evidence that the Great Pacific Garbage Patch is rapidly accumulating plastic. *Scientific Reports*, *8*(1), 1–15. https://doi.org/10.1038/s41598-018-22939-w

Liu, P., Zhan, X., Wu, X., Li, J., Wang, H., & Gao, S. (2020). Effect of weathering on environmental behavior of microplastics: Properties, sorption and potential risks. *Chemosphere*, *242*, 125193. https://doi.org/10.1016/j.chemosphere.2019.125193

Lobelle, D., & Cunliffe, M. (2011). Early microbial biofilm formation on marine plastic debris. *Marine Pollution Bulletin*, *62*(1), 197–200. https://doi.org/10.1016/j.marpolbul.2010.10.013

Lodish, H., Berk, A., Zipursky, L., Matsudaira, P., Baltimore, D., & Darnell, J. (2000). *Molecular Cell Biology* (4th ed.).

Majorek, K. A., Porebski, P. J., Dayal, A., Zimmerman, M. D., Jablonska, K., Stewart, A. J., Chruszcz, M., & Minor, W. (2012). Structural and immunologic characterization of bovine, horse, and rabbit serum albumins. *Molecular Immunology*, *52*(3–4), 174–182. https://doi.org/10.1016/j.molimm.2012.05.011

Malmsten, M., & Alstine, J. A. (1996). *Adsorption of Poly (Ethylene Glycol) Amphiphiles to Form Coatings Which Inhibit Protein Adsorption*. *512*(177), 502–512.

Martins de Oliveira, V., Godoi Contessoto, V. de, Bruno da Silva, F., Zago Caetano, D. L.,

Jurado de Carvalho, S., & Pereira Leite, V. B. (2018). Effects of pH and Salt Concentration on Stability of a Protein G Variant Using Coarse-Grained Models. *Biophysical Journal*, *114*(1), 65–75. https://doi.org/10.1016/j.bpj.2017.11.012

Masó, M., Garcés, E., Pagès, F., & Camp, J. (2003). Drifting plastic debris as a potential vector for dispersing Harmful Algal Bloom (HAB) species. *Scientia Marina*, *67*(1), 107–111. https://doi.org/10.3989/scimar.2003.67n1107

Maurer-Jones, M. A., & Monzo, E. M. (2021). Quantifying Photochemical Transformations of Poly(butylene adipate- co-terephthalate) Films. *ACS Applied Polymer Materials*, *3*(2), 1003–1011. https://doi.org/10.1021/acsapm.0c01283

Moreno-Gonzalez, I., & Soto, C. (2012). Potential for Disease Transmission. *Semin Cell Dev Biol*, *22*(5), 482–487. https://doi.org/10.1016/j.semcdb.2011.04.002.Misfolded

O'Connor, C., & Adams, C. . (2010). *Essentials of Cell Biology*. Cambridge.

Pabbathi, A., Patra, S., & Samanta, A. (2013). Structural transformation of bovine serum albumin induced by dimethyl sulfoxide and probed by fluorescence correlation spectroscopy and additional methods. *ChemPhysChem*, *14*(11), 2441–2449. https://doi.org/10.1002/cphc.201300313

Pace, N., Scholtz, M., & Grimsley, G. (2015). *Pace_proteín stability_2014.pdf*. *588*(14), 2177–2184. https://doi.org/10.1016/j.febslet.2014.05.006.Forces

Parker, M. W. (2003). Protein Structure from X-Ray Diffraction. *Journal of Biological Physics*, *29*(4), 341–362. https://doi.org/10.1023/A:1027310719146

Pleshakova, T. O., Bukharina, N. S., Archakov, A. I., & Ivanov, Y. D. (2018). Atomic force microscopy for protein detection and their physicochemical characterization. *International Journal of Molecular Sciences*, *19*(4). https://doi.org/10.3390/ijms19041142

Rabe, M., Verdes, D., & Seeger, S. (2011). Understanding protein adsorption phenomena at solid surfaces. *Advances in Colloid and Interface Science*, *162*(1–2), 87–106. https://doi.org/10.1016/j.cis.2010.12.007

Rabek, J. (1995). *Polymer Photodegradation*. Springer Netherlands.

Ratner, B., Hoffman, A., Schoen, F., & Lemons, J. (2012). *Biomaterials Science*. Academic Press.

Roman, L., Kastury, F., Petit, S., Aleman, R., Wilcox, C., Hardesty, B. D., & Hindell, M. A. (2020). Plastic, nutrition and pollution; relationships between ingested plastic and metal concentrations in the livers of two Pachyptila seabirds. *Scientific Reports*, *10*(1), 1–14. https://doi.org/10.1038/s41598-020-75024-6

Royer, C. (1995). *Fluorescence Spectroscopy*. Humana Press.

Schuurmans Stekhoven, F. M. A. H., Gorissen, M. H. A. G., & Flik, G. (2008). The isoelectric point, a key to understanding a variety of biochemical problems: A minireview. *Fish Physiology and Biochemistry*, *34*(1), 1–8. https://doi.org/10.1007/s10695-007-9145-6

Shyichuk, A. V., & White, J. R. (2000). Analysis of chain-scission and crosslinking rates in the photo-oxidation of polystyrene. *Journal of Applied Polymer Science*, *77*(13), 3015–3023. https://doi.org/10.1002/1097-4628(20000923)77:13<3015::AID-APP28>3.0.CO;2-W

Singh, A. (1999). Irradiation of polyethylene: Some aspects of crosslinking and oxidative degradation. *Radiation Physics and Chemistry*, *56*(4), 375–380. https://doi.org/10.1016/S0969-806X(99)00328-X

Singh, S., Singh, S. K., Chowdhury, I., & Singh, R. (2017). Understanding the Mechanism of Bacterial Biofilms Resistance to Antimicrobial Agents. *The Open Microbiology Journal*, *11*(1), 53–62. https://doi.org/10.2174/1874285801711010053

Sneha, P., & Priya Doss, C. G. (2016). Molecular Dynamics: New Frontier in Personalized Medicine. In *Advances in Protein Chemistry and Structural Biology* (1st ed., Vol. 102). Elsevier Inc. https://doi.org/10.1016/bs.apcsb.2015.09.004

Spillers, C., Wriggers, W., & He, J. (2017). Detection of Protein Secondary Structure Patterns from 3D Cryo-TEM Maps at Medium Resolution - Combining the Best of SSETracer and VolTrac. *Microscopy and Microanalysis*, *23*(S1), 242–243. https://doi.org/10.1017/s1431927617001891

Sukumaran, S. (2018). *Protein secondary structure elucidation using FTIR spectroscopy*. 4.

Sun, Y., Yuan, J., Zhou, T., Zhao, Y., Yu, F., & Ma, J. (2020). Laboratory simulation of microplastics weathering and its adsorption behaviors in an aqueous environment: A systematic review. *Environmental Pollution*, *265*, 114864. https://doi.org/10.1016/j.envpol.2020.114864

Thompson, R. C., Moore, C. J., Saal, F. S. V., & Swan, S. H. (2009). Plastics, the environment and human health: Current consensus and future trends. *Philosophical Transactions of the Royal Society B: Biological Sciences*, *364*(1526), 2153–2166. https://doi.org/10.1098/rstb.2009.0053

Thyparambil, A. A., Wei, Y., & Latour, R. A. (2015). Experimental characterization of adsorbed protein orientation, conformation, and bioactivity. *Biointerphases*, *10*(1), 019002. https://doi.org/10.1116/1.4906485

Tomer, N. S., Delor-Jestin, F., Frezet, L., & Lacoste, J. (2012). Oxidation, Chain Scission and Cross-Linking Studies of Polysiloxanes upon Ageings. *Open Journal of Organic Polymer Materials*, *02*(02), 13–22. https://doi.org/10.4236/ojopm.2012.22003

Velzeboer, I., Kwadijk, C. J. A. F., & Koelmans, A. A. (2014). Strong sorption of PCBs to

nanoplastics, microplastics, carbon nanotubes, and fullerenes. *Environmental Science and Technology*, *48*(9), 4869–4876. https://doi.org/10.1021/es405721v

Verma, R., Vinoda, K. S., Papireddy, M., & Gowda, A. N. S. (2016). Toxic Pollutants from Plastic Waste- A Review. *Procedia Environmental Sciences*, *35*, 701–708. https://doi.org/10.1016/j.proenv.2016.07.069

Whited, A. M., & Park, P. S. H. (2014). Atomic force microscopy: A multifaceted tool to study membrane proteins and their interactions with ligands. *Biochimica et Biophysica Acta - Biomembranes*, *1838*(1 PARTA), 56–68. https://doi.org/10.1016/j.bbamem.2013.04.011

Zhang, L., Liu, B., Li, Z., & Guo, Y. (2015). Study on interaction between cefixime and bovine serum albumin by modified fluorescence spectroscopy. *Asian Journal of Chemistry*, *27*(4), 1449–1452. https://doi.org/10.14233/ajchem.2015.18289

Zhang, W., Ang, W. T., Xue, C. Y., & Yang, K. L. (2011). Minimizing nonspecific protein adsorption in liquid crystal immunoassays by using surfactants. *ACS Applied Materials and Interfaces*, *3*(9), 3496–3500. https://doi.org/10.1021/am200716x